

Supernova equations of state including full nuclear ensemble with in-medium effects

Shun Furusawa^{a,b}, Kohsuke Sumiyoshi^c, Shoichi Yamada^d, Hideyuki Suzuki^e

^a*Frankfurt Institute for Advanced Studies, J.W. Goethe University, 60438 Frankfurt am Main, Germany*

^b*Center for Computational Astrophysics, National Astronomical Observatory of Japan, Osawa, Mitaka, Tokyo, 181-8588, Japan*

^c*Numazu College of Technology, Ooka 3600, Numazu, Shizuoka 410-8501, Japan*

^d*Department of Science and Engineering, Waseda University, 3-4-1 Okubo, Shinjuku, Tokyo 169-8555, Japan*

^e*Faculty of Science and Technology, Tokyo University of Science, Yamazaki 2641, Noda, Chiba 278-8510, Japan*

Abstract

We construct new equations of state for baryons at sub-nuclear densities for the use in core-collapse supernova simulations. The abundance of various nuclei is obtained together with thermodynamic quantities. The formulation is an extension of the previous model, in which we adopted the relativistic mean field theory with the TM1 parameter set for nucleons, the quantum approach for d , t , h and α as well as the liquid drop model for the other nuclei under the nuclear statistical equilibrium. We reformulate the model of the light nuclei other than d , t , h and α based on the quasi-particle description. Furthermore, we modify the model so that the temperature dependences of surface and shell energies of heavy nuclei could be taken into account. The pasta phases for heavy nuclei and the Pauli- and self-energy shifts for d , t , h and α are taken into account in the same way as in the previous model. We find that nuclear composition is considerably affected by the modifications in this work, whereas thermodynamical quantities are not changed much. In particular, the washout of shell effect has a great impact on the mass distribution above $T \sim 1$ MeV. This improvement may have an important effect on the rates of electron captures and coherent neutrino scatterings on nuclei in supernova cores.

Keywords: equation of state, core-collapse supernova

1. Introduction

Hot and dense matter can be realized in core collapse supernovae, which occur at the end of the evolution of massive stars and lead to the formations of a neutron star or a black hole, the emissions of neutrinos and gravitational waves and the synthesis of heavy elements. The mechanism of this event is not clearly understood yet because of their intricacies (see e.g. Janka (2012); Kotake et al. (2012); Burrows (2013)). One of the underlying problems in these events is the equations of state (EOS's) of hot and dense matter both at sub- and supra-nuclear densities. EOS provides information on compositions of nuclear matter in addition to thermodynamical quantities such as pressure, entropy and sound velocity. The compositions play important roles to determine the evolution of the lepton fraction through weak interactions. This lepton fraction is one of the most critical ingredients for the dynamics of core collapse supernovae (Hix et al., 2003; Lentz et al., 2012).

The EOS for the simulations of core collapse supernovae must cover a wide range of density ($10^5 \lesssim \rho_B \lesssim 10^{15} \text{g/cm}^3$) and temperature ($0.1 \lesssim T \lesssim 10^2 \text{ MeV}$), including both neutron-rich and proton-rich regimes. One of the difficulties in constructing the EOS is originated from the fact that depending on the density, temperature and proton fraction, the matter consists of either dilute free nucleons or a mixture of nuclei and free nucleons or strongly interacting dense nucleons. Furthermore, there are uncertainties not only in the description of homogeneous matter but also of the in-medium effect for nuclei at finite densities and temperatures (Aymard et al., 2014; Agrawal et al., 2014). The fact makes the variation of supernova EOS's (Steiner et al., 2013; Buyukcizmeci et al., 2013). At high temperatures ($T \gtrsim 0.4 \text{ MeV}$), chemical equilibrium is achieved for all strong and electromagnetic reactions, which is referred to as nuclear statistical equilibrium and the nuclear composition is determined as a function of density, temperature, and proton fraction (Timmes and Arnett, 1999; Blinnikov et al., 2011). In this paper, we are concerned with the high temperature regime, in which the nuclear composition can be treated as a part of EOS.

There are two types of EOSs for supernova simulations. The single nucleus approximation (SNA) is the one option, in which the ensemble of heavy nuclei is represented by a single nucleus. The other option is multi-nucleus EOS, in which thermal ensemble of various nuclei is solved for each set up of thermodynamical condition. Two standard EOS's in wide use for the simulations of core-collapse supernovae are categorized to the former group;

Lattimer and Swesty (1991) and Shen et al. (1998a,b); Shen et al. (2011) calculated the representative heavy nuclei by using the compressible liquid drop model and Thomas Fermi model, respectively. In such calculations, in-medium effects on a single nucleus, such as compression and deformation, are taken into account more easily in comparison with the multi-nucleus EOS. On the other hand, they can never provide a nuclear composition, which is indispensable to estimate weak interaction rates in supernova simulations. Furthermore, even the average mass number and total mass fraction of heavy nuclei may not be correctly reproduced by the representative nucleus due to the SNA approximation (Burrows and Lattimer, 1984; Hempel and Schaffner-Bielich, 2010; Furusawa et al., 2011).

In this decade, some multi-nucleus EOS's have been formulated by different research groups. SMSM EOS (Botvina and Mishustin, 2004, 2010; Buyukcizmeci et al., 2014) is a generalization of the statistical model of multi-fragmentation reactions induced by heavy-ion collisions (Bondorf et al., 1995). In this model, temperature dependences of bulk and surface energies are taken into account based on the liquid drop model (LDM) although they ignored the shell effects of nuclei, which are important for reproducing the abundance of nuclei at low temperatures. Hempel and Schaffner-Bielich (2010) also construct EOS's (HS EOS) based on the relativistic mean field theory (RMF) with different parameters for nuclear interactions. In this model, nuclear binding energies as well as shell effects are evaluated from experimental and theoretical mass data in vacuum. They ignored, on the other hand, high-density and -temperature effects on nuclear bulk, surface and shell energies, which are explained later. The EOS provided by G. Shen et al. (Shen et al., 2011) is a hybrid model, where a multi-nucleus EOS based on the Virial expansion with multi-nucleus at low densities is switched to a single-nucleus EOS via Hartree approximation at high densities, i.e., the multi-nucleus description is employed only in the low density regime and, as a result, some quantities are discontinuous or non-smooth at the transition between the two descriptions.

We constructed in the previous papers (Furusawa et al., 2011, 2013) an EOS based on the mass formula for nuclei under the influence of surrounding nucleons and electrons. The mass formula extended from the LDM to describe nuclear shell effects as well as various in-medium effects, in particular, the formation of the pasta phases (Watanabe et al., 2005; Newton and Stone, 2009; Okamoto et al., 2012). The binding energies of d (deuteron), t (triton), h (He^3) and α (He^4) are estimated with a quantum approach to light clusters

(Typel et al., 2010; Röpke, 2009). Other light nuclei ($Z \leq 5$) are described with another mass formula based on the LDM, which is different from the one for heavy nuclei. The details of the model and comparisons with H. Shen’s EOS and HS EOS are given in Furusawa et al. (2011). In Buyukcizmeci et al. (2013), three multi-nucleus EOS’s (SMSM, HS and ours) were compared in detail. The extension of shell effects and the implementation of the temperature dependence in bulk energies for heavy nuclei and the introduction of the quantum approach to d , t , h and α were reported in Furusawa et al. (2013).

The purpose of this study is to further improve the previous model, in which temperature dependences of binding energies are lacked in part, and to discuss their impact on EOS systematically. Most significant change is the introduction of the washout of shell effects at high temperatures. It is pointed out by experimental and theoretical studies that nuclear shell effects disappear completely at $T \sim 2.0 - 3.0$ MeV (Brack and Quentin, 1974; Bohr and Mottelson, 1998; Sandulescu et al., 1997; Nishimura and Takano, 2014). All supernova EOS’s with multi-nucleus, however, have not considered this effect. In SMSM EOS, shell effects are ignored from the beginning and completely washed out even at zero temperature. Other multi-nucleus EOS’s including our previous model assume full shell effects at any temperature. The shell effects are known to affect the nuclear abundance and electron capture rates of heavy nuclei to a great extent (Buyukcizmeci et al., 2013; Raduta et al., 2016). Other improvements are the introduction of the surface tension in its temperature dependence and the reformulation of model for light nuclei other than d , t , h and α . In the following, we report on these new ingredients and discuss the differences from the previous version.

This article is organized as follows. In section 2, we describe our new model with a focus on the development from the previous EOS. Note that the basic formulation of the model free energy and its minimization are unchanged from the previous version. The results are shown in section 3, with an emphasis on the impact of the temperature dependence in binding energies. The paper is wrapped up with a summary and some discussions in section 4. In appendix, the data table of this EOS is explained for use in supernova simulations.

2. Formulation of the model

To obtain the EOS with multi-nucleus, we construct a model free energy to be minimized with respect to the parameters included. The supernova

matter consists of nucleons and nuclei together with electrons, photons and neutrinos. Electrons and photons are not treated in this paper, since their inclusion as ideal Fermi and Bose gases, respectively, is trivial. Note that the Coulomb energies between protons, both inside and outside nuclei, and electrons are contained in the EOS. We assume the electrons are uniformly distributed. Neutrinos are not always in thermal or chemical equilibrium with matter. We do not include them in the free energies.

The free energy of our model is constructed as a sum of the contributions from free nucleons not bound in nuclei, light nuclei defined here as those nuclei with the proton number $Z \leq 5$, and the rest of heavy nuclei with the proton and neutron numbers, $Z \leq 1000$ and $N \leq 1000$. We assume that the free nucleons outside nuclei interact with themselves only in the volume that is not occupied by other nuclei; light nuclei are the quasi particles whose masses are modified by the surrounding free nucleons; heavy nuclei are also affected by the free nucleons and electrons, depending on the temperature and density. The free energy of free nucleons is calculated by the RMF theory with the excluded volume effect being taken into account. The model free energy of heavy nuclei is based on the liquid drop mass formula taking the following issues into account: the nuclear masses at low densities and temperatures should be equal to those of isolated nuclei in vacuum; one should take into account the effect that the nuclear bulk, shell, Coulomb and surface energies are affected by the free nucleons and electrons at high densities and temperatures; furthermore the pasta phases near the saturation densities should be also accounted for to ensure a continuous transition to uniform matter. The free energy of light nuclei is approximately calculated by quantum many body theory.

In the following subsections, we explain the details of the free energy density,

$$f = f_{p,n} + \sum_j n_j F_j + \sum_i n_i F_i, \quad (1)$$

$$F_{j/i} = E_{j/i}^t + M_{j/i}, \quad (2)$$

where $f_{p,n}$ is the free energy densities of free nucleons, $n_{j/i}$, $F_{j/i}$, $E_{j/i}^t$ and $M_{j/i}$ are the number density, free energy, translational energy and rest mass of individual nucleus and indices j and i specify light and heavy nuclei, respectively. The modifications from our previous EOS (Furusawa et al., 2013) are temperature dependences of shell and surface energies and the

model of the light nuclei ($Z_j \leq 5$) other than d, t, h and α such as ${}^7\text{Li}$. The other parts in free energies and the minimization of the total free energy densities are just the same as in the previous paper (Furusawa et al., 2013).

2.1. minimization of free energy

The thermodynamical quantities and abundances of nuclei as a function of ρ_B , T and Y_p are obtained by minimizing the model free energy with respect to the number densities of nuclei and nucleons under the constraints,

$$\begin{aligned} n_p + n_n + \sum_j A_j n_j + \sum_i A_i n_i &= n_B = \rho_B / m_u, \\ n_p + \sum_j Z_j n_j + \sum_i Z_i n_i &= n_e = Y_p n_B, \end{aligned} \quad (3)$$

where n_B and n_e are number densities of baryon and electrons, $A_{j/i}$ and $Z_{j/i}$ are the mass and proton numbers of nucleus j/i and m_u is the atomic mass unit. The minimization of our free energy density is not the same as that in the ordinary NSE, in which the number densities of all nuclei as well as nucleons are expressed by two variable, i.e., the chemical potentials of nucleons μ_p and μ_n and one has only to solve the constraints, Eq. (3) for the two variables, through Saha equations. In our case, on the other hand, the free energy density of nuclei depends on the local number densities of proton and neutron $n'_{p/n}$ to evaluate in-medium effects accurately and μ_p and μ_n are expressed as follows:

$$\mu_{p/n} = \frac{\partial f}{\partial n_{p/n}} = \mu'_{p/n}(n'_p, n'_n) + \sum_{i/j} n_{i/j} \frac{\partial F_{i/j}(n'_p, n'_n)}{\partial n_{p/n}}, \quad (4)$$

where $\mu'_{p/n}$ is the chemical potentials of nucleons in the vapor (see section 2.2) and the second term is originated from the dependence of the free energies of nuclei on the nucleon densities in the vapor (see sections 2.3 and 2.4) and hence is summed over all nuclear species. Thus the number densities of nuclei are not determined by μ_p and μ_n alone but they also depend on n'_p and n'_n . We hence solve the equations relating $\mu_{p/n}$ and $n'_{p/n}$, Eq. (4), as well as the two constraint equations, Eq. (3), to determine the four variables: μ_p , μ_n , n'_p and n'_n .

2.2. free energy for nucleons outside nuclei

The free energy density of free nucleons is calculated by the RMF theory with the TM1 parameter set, which is determined so that it should reproduce the properties of heavy nuclei in the wide mass range including neutron rich nuclei, and is the same as that adopted in Shen et al. (2011). We take into account the excluded-volume effect: free nucleons can not move in the volume occupied by other nuclei, V_N . Then the local number densities of free protons and neutrons are defined as $n'_{p/n} = (N_{p/n})/(V - V_N)$ with the total volume, V , and the numbers of free protons, N_p , and free neutrons, N_n . Then the free energy densities of free nucleons are defined as $f_{p,n} = (V - V_N)/V \times f^{RMF}(n'_p, n'_n, T)$, where $f^{RMF}(n'_p, n'_n, T)$ is the free energy density in the unoccupied volume for nucleons, $V - V_N$, obtained from the RMF theory at n'_p , n'_n and temperature T .

2.3. masses of heavy nuclei ($Z \geq 6$)

The nuclear mass is assumed to be the sum of bulk, Coulomb, surface and shell energies: $M_i = E_i^B + E_i^C + E_i^{Su} + E_i^{Sh}$. The formulation of bulk and Coulomb energies is just identical to the previous one. In the new model, we take into account the temperature dependences of shell and surface energies.

We define the saturation densities of nuclei $n_{si}(T)$ as the baryon number density, at which the free energy per baryon $F^{RMF}(T, n_B, Y_p)$ given by the RMF with $Y_p = Z_i/A_i$ takes its minimum value. Thus $n_{si}(T)$ depends on the temperature T and the proton fraction in each nucleus Z_i/A_i . At temperatures larger than a critical temperature T_{ci} , the free energy, $F^{RMF}(T, n_B, Z_i/A_i)$, has no minimum because of the entropy contribution. Then the saturation density $n_{si}(T)$ above T_{ci} is assumed to be equal to the saturation density at the critical temperature $n_{si}(T_{ci})$. When the saturation density n_{si} so obtained is lower than the baryon number density of the whole system n_B , we reset the saturation density as the baryon number density $n_{si} = n_B$. This prescription approximately represents compressions of nuclei near the saturation densities. These treatments of the saturation density are important in obtaining reasonable bulk energies at high temperatures and densities (Furusawa et al., 2011, 2013). The bulk energies are evaluated from the free energy per baryon of the uniform nuclear matter at the saturation density n_{si} for a given temperature T and proton fraction inside the nucleus Z_i/A_i as $E_i^B = A_i\{M_B + F^{RMF}(T, n_{si}, Z_i/A_i)\}$, where the baryon mass M_B is set to be 938 MeV.

The Wigner-Seitz cell (W-S cell) for each species of nuclei is set to satisfy charge neutrality with the volume, V_i . The cell also contains free nucleons as a vapor outside the nucleus as well as electrons distributed uniformly in the entire cell. The charge neutrality in the cell gives the cell volume $V_i = (Z_i - n'_p V_i^N)/(n_e - n'_p)$ where V_i^N is the volume of the nucleus in the cell and can be calculated as $V_i^N = A_i/n_{si}$. The vapor volume and nucleus volume fraction in the cell are given by $V_i^B = V_i - V_i^N$ and $u_i = V_i^N/V_i$, respectively. In this EOS, we assume that each nucleus enters the nuclear pasta phase individually when the volume fraction reaches $u_i = 0.3$ and that the bubble shape is realized when it exceeds 0.7. The bubbles are explicitly treated as nuclei of spherical shell shapes with the vapor nucleons filling the inside. This phase is important to ensure continuous transitions to uniform matter as noted in Furusawa et al. (2011). The intermediate states ($0.3 < u_i < 0.7$) are smoothly interpolated from the normal and bubble states. The evaluation of the Coulomb energy in the W-S cell is given by the integration of Coulomb forces in the cell:

$$E_i^C = \begin{cases} \frac{3}{5} \left(\frac{3}{4\pi} \right)^{-1/3} e^2 n_{si}^2 \left(\frac{Z_i - n'_p V_i^N}{A_i} \right)^2 V_i^{N5/3} D(u_i) & (u_i \leq 0.3), \\ \frac{3}{5} \left(\frac{3}{4\pi} \right)^{-1/3} e^2 n_{si}^2 \left(\frac{Z_i - n'_p V_i^N}{A_i} \right)^2 V_i^{B5/3} D(1 - u_i) & (u_i \geq 0.7), \end{cases} \quad (5)$$

with $D(u_i) = 1 - \frac{3}{2}u_i^{1/3} + \frac{1}{2}u_i$, where e is the elementary charge.

The surface energies are evaluated as

$$E_i^{Su} = \begin{cases} 4\pi r_{Ni}^2 \sigma_i \left(1 - \frac{n'_p + n'_n}{n_{si}} \right)^2 \left(\frac{T_c^2 - T^2}{T_c^2 + T^2} \right)^{5/4} & (u_i \leq 0.3), \\ 4\pi r_{Bi}^2 \sigma_i \left(1 - \frac{n'_p + n'_n}{n_{si}} \right)^2 \left(\frac{T_c^2 - T^2}{T_c^2 + T^2} \right)^{5/4} & (u_i \geq 0.7), \end{cases} \quad (6)$$

$$\sigma_i = \sigma_0 - \frac{A_i^{2/3}}{4\pi r_{Ni}^2} [S_s (1 - 2Z_i/A_i)^2], \quad (7)$$

where $r_{Ni} = (3/4\pi V_i^N)^{1/3}$ and $r_{Bi} = (3/4\pi V_i^B)^{1/3}$ are the radii of nucleus and bubble and σ_0 denotes the surface tension for symmetric nuclei. The surface tension σ_i includes the surface symmetry energy, i.e., neutron-rich nuclei have lower surface tensions than symmetric nuclei. The values of the constants, $\sigma_0 = 1.15 \text{ MeV/fm}^3$ and $S_s = 45.8 \text{ MeV}$, are adopted from the paper by

Lattimer and Swesty (1991). The factor in Eq. (6), $(1 - (n'_p + n'_n)/n_{si})^2$, is added by hand to take into account the effect that the surface energy should be reduced as the density contrast decreases between the nucleus and the nucleon vapor. The last factor in Eq. (6), $((T_c^2 - T^2)/(T_c^2 + T^2))^{5/4}$, accounts for the temperature dependence in the surface tension and is one of the improvements in the new model. This factor reproduces approximately the liquid-gas phase transition at the critical temperature $T_c = 18$ MeV, where the nuclei are dissolved to free nucleons (Ravenhall et al., 1983; Bondorf et al., 1995). This factor is also adopted in the SMSM EOS (Botvina and Mishustin, 2004, 2010; Buyukcizmeci et al., 2014). Note that the values of σ_i and T_c are not consistent with the RMF theory with the TM1 parameter set and the dependence of T_c on the proton fraction in each nucleus Z_i/A_i is not taken into account for simplicity. We use cubic polynomials of u_i for the interpolation between the droplet and bubble phases. The four coefficients of the polynomials are determined by the condition that the Coulomb and surface energies are continuous and smooth as a function of u_i at $u_i = 0.3$ and $u_i = 0.7$.

We include the shell effects separately in the mass formula of nuclei by the use of both experimental and theoretical mass data (Audi et al., 2012; Koura et al., 2005) to better reproduce the nuclear abundances in the low density regime. The shell energies are obtained from the mass data by subtracting our liquid drop mass formula, which does not include the shell effects, ($M_i^{LDM} = E_i^B + E_i^C + E_i^{Su}$) in the vacuum limit with $T, n'_p/n, n_e = 0$ as $E_{i0}^{Sh} = M_i^{data} - [M_i^{LDM}]_{vacuum}$. Note that the shell energy in our mass formula actually includes pair energies. We take the in-medium effect into account phenomenologically as follows:

$$E_i^{Sh}(\rho, T) = \begin{cases} E_{i0}^{Sh} \frac{\tau_i}{\sinh \tau_i} & (\rho \leq 10^{12} \text{g/cm}^3), \\ E_{i0}^{Sh} \left(\frac{\tau_i}{\sinh \tau_i} \right) \left(\frac{\rho_0 - \rho}{\rho_0 - 10^{12} \text{g/cm}^3} \right) & (\rho > 10^{12} \text{g/cm}^3), \end{cases} \quad (8)$$

where ρ_0 is taken to be m_u times the saturation density of symmetric nuclei $n_{si}(T, Z_i/A_i = 0.5)$ at temperature T . The factor $\tau_i/\sinh \tau_i$ expresses the washout of shell effects approximately, which is derived by the analytical study for the single particle motion of nucleon outside the closed shell (Bohr and Mottelson, 1998). The normalized factor τ_i is defined as $\tau_i = 2\pi^2 T / \epsilon_i^{sh}$ with the energy spacing of the shells, $\epsilon_i^{sh} = 41 A_i^{-1/3}$ MeV. Note that E_0^{Sh} and ϵ_i^{sh} are not based on exact calculations of nuclear struc-

tures but the simple assumptions and in this sense, this formulation of the washout is an approximation. The fully self-consistent calculation with the nuclear composition and structures of all nuclei including in-medium effects is much beyond the scope of this study. It is noted that this approximate formulation can reproduce qualitatively the feature of washout that the shell effects disappear around $T \sim 2.0\text{-}3.0$ MeV as shown later in Sec 3. The linear interpolation, $(\rho_0 - \rho_B)/(\rho_0 - 10^{12}\text{g/cm}^3)$, accounts for the decay of shell effects at high densities because of the existence of electrons, free nucleons and other nuclei. This disappearance of shell energies is essential for our EOS model to reproduce continuous transition to the uniform nuclear matter at saturation densities (Furusawa et al., 2011). The choice of the critical density 10^{12}g/cm^3 is rather arbitrary, since the dependence of the shell energies on the density of ambient matter has not been thoroughly investigated yet. It is noted, however, that the structure of nuclei is known to be affected by ambient matter at these densities (Aymard et al., 2014).

2.4. masses of light nuclei ($Z \leq 5$)

We describe light nuclei as quasi-particles outside heavy nuclei. Their masses are assumed to be given by the following expression:

$$M_j = M_j^{data} + \Delta E_j^{Pa} + \Delta E_j^{SE} + \Delta E_j^C \quad (j = d, t, h \ \& \ \alpha), \quad (9)$$

where ΔE_j^{Pa} is the Pauli energy shift by other baryons, ΔE_j^{SE} is the self-energy shift of the nucleons composing the light nuclei and ΔE_j^C is the Coulomb energy shift.

For the Pauli energy shifts of d, t, h and α , we employ the empirical formulae provided by Typel et al. (2010), which are quadratic functions fitted to the result of quantum statistical calculations (Röpke, 2009). The local proton and neutron number densities that include light nuclei are defined as

$$n_{pl} = n'_p + \eta^{-1} \sum_j Z_j n_j, \quad (10)$$

$$n_{nl} = n'_n + \eta^{-1} \sum_j N_j n_j. \quad (11)$$

where η stands for the volume fraction $(V - V_N)/V$. Then the Pauli energy shift ΔE_j^{Pa} is given by the following expression (Typel et al., 2010):

$$\Delta E_j^{Pa}(n_{pl}, n_{nl}, T) = -\tilde{n}_j \left[1 + \frac{\tilde{n}_j}{2\tilde{n}_j^0(T)} \right] \delta B_j(T), \quad (12)$$

$$\delta B_j(T) = \begin{cases} a_{j,1}/T^{3/2} [1/\sqrt{y_j} - \sqrt{\pi}a_{j,3} \exp(a_{j,3}^2 y_j) \operatorname{erfc}(a_{j,3}\sqrt{y_j})] & \text{for } j = d, \\ a_{j,1}/(T y_j)^{3/2} & \text{for } j = t, h, \alpha, \end{cases} \quad (13)$$

where $\tilde{n}_j = 2(Z_j n_{pl} + N_j n_{nl})/A_j$ and $y_j = 1 + a_{j,2}/T$. The density scale for the dissolution of each light nucleus is given by $\tilde{n}_j^0(T) = B_j^0/\delta B_j(T)$ with the binding energy in vacuum, $B_j^0 = Z_j M_p + N_j M_n - M_j^{data}$.

The self-energy shifts of light nuclei are the sum of the self-energy shifts of individual nucleons composing the light nuclei $\Delta E_{n/p}^{SE} = \Sigma_{n/p}^0(T, n'_p, n'_n) - \Sigma_{n/p}(T, n'_p, n'_n)$ with Σ^0 and Σ being the vector and scalar potentials of nucleon and the contribution from their effective masses $\Delta E_j^{\text{eff.mass}}$:

$$\Delta E_j^{SE}(n'_p, n'_n, T) = (A_j - Z_j)\Delta E_n^{SE} + Z_j\Delta E_p^{SE} + \Delta E_j^{\text{eff.mass}}. \quad (14)$$

The latter is given as $\Delta E_j^{\text{eff.mass}} = (1 - m^*/m) s_j$ with $m^* = m_B - \Sigma_{n/p}(T, n'_p, n'_n)$. The potentials Σ^0 and Σ are calculated from the RMF employed for free nucleons as noted in 2.2. More detailed explanations of the Pauli- and self-energy shifts of d, t, h and α are provided in Typel et al. (2010); Röpke (2009); Furusawa et al. (2013). The parameters $a_{j,1}$, $a_{j,2}$, $a_{j,3}$, and s_j are given in Table 1 in Furusawa et al. (2013).

There is little information about the in-medium effects for the light nuclei ($Z_j \leq 5$) other than d, t, h and α . In the previous model, their binding energies are evaluated with the LDM that is different from the one for heavy nuclei. Their bulk energies are linearly interpolated between the two different estimations at $\rho_B = 10^{12}$ g/cm³ and at the nuclear saturation density: at the lower end, they are evaluated from the experimental or theoretical mass data in the vacuum limit; at the other end they are designed to agree with the bulk energies for heavy nuclei in the same LDM. The light nuclei are assumed to form nuclear pastas together with heavy nuclei ($Z \geq 6$) near the saturation densities. It is noted, however, that there is no justification for this interpolation. For simplicity these light nuclei are assumed to be quasi particles in the same way as d, t, h and α at all sub-nuclear densities and their mass are evaluated with Eq. (9) in the new model. The Pauli-energy shifts for them are calculated with Eq. (12) in the same way as that for α . The self-energy shifts for them are set to be zero, on the other hand. This reformulation has only minor influence on the nuclear composition and thermodynamical quantities, since the light nuclei other than d, t, h and α do not become abundant as shown later. This is because they have smaller binding energies than α and are less populated than d, t, h and α at high temperatures, which give higher entropies per baryon.

The Coulomb energy shifts are calculated as

$$\Delta E_j^C = E_j^C(n'_p, u_j) - E_j^C(0, 0), \quad (15)$$

where E_j^C is given as

$$E_j^C(n'_p, u_j) = \frac{3}{5} \left(\frac{3}{4\pi} \right)^{-1/3} e^2 n_{sj}^2 \left(\frac{Z_j - n'_p V_j^N}{A_j} \right)^2 V_j^{N^{5/3}} D(u_j). \quad (16)$$

Although the expression of the Coulomb energy is identical to that for heavy nuclei, the shifts are negligible compared with other energy shifts. We do not take into account the nuclear pasta phases and surface- and shell-energies both for d , t , h and α and for the rest of light nuclei.

2.5. Translational energies of nuclei

The translational energy of nucleus i in our model free energy is based on that for the ideal Boltzmann gas and given by

$$F_{i/j}^t = k_B T \left\{ \log \left(\frac{n_{i/j}}{g_{i/j}(T) n_{Q_{i/j}}} \right) - 1 \right\} \left(1 - \frac{n_B}{n_s} \right), \quad (17)$$

where k_B is the Boltzmann constant and $n_{Q_{i/j}} = (M_{i/j} k_B T / 2\pi \hbar^2)^{3/2}$. We modify the internal degree of freedom $g_{i/j}(T)$ for heavy nuclei in this paper so that it should approach unity in line with the washout of the shell effects: $g_i(T) = (g_i^0 - 1) \frac{\tau_i}{\sinh \tau_i} + 1$. In the previous model, we just used the spin degree of freedom of the ground state as $g_i(T) = g_i^0$ at any temperature. Note that the contribution of the excited states to free energy is included in the temperature dependence of the bulk energy. As for light nuclei, g_j^0 is always adopted. The last factor on the right hand side of Eq. (17) takes account of the excluded-volume effect: each nucleus can move in the space that is not occupied by other nuclei and free nucleons in the same way as in Lattimer and Swesty (1991). The factor reduces the translational energy at high densities and is important to ensure the continuous transition to uniform nuclear matter. We always employ the nuclear saturation density of symmetric matter $n_s = [n_{si}(Z_i/A_i, T)]_{Z_i/A_i=0.5}$ in Eq. (17) for numerical convenience.

2.6. Thermodynamical quantities

By minimization, we obtain the free energy density together with the abundances of all nuclei and free nucleons as a function of ρ_B , T and Y_p . Other physical quantities are derived by partial differentiations of the optimized free energy density. All the terms for the in-medium effects are properly taken into account in this process to ensure the thermodynamical consistency as described in Furusawa et al. (2011) in detail. The baryonic pressure, for example, is obtained by the differentiation with respect to the baryonic density as follows:

$$\begin{aligned} p_B &= n_B [\partial f / \partial n_B]_{T, Y_e} - f, \\ &= p_{p,n}^{RMF} + \sum_{i/j} (p_{i/j}^{th} + p_{i/j}^{ex} + p_{i/j}^{mass}), \end{aligned} \quad (18)$$

$$p_i^{mass} = (p_i^{shell} + p_i^{Coul} + p_i^{Surf}) \quad (\text{heavy nuclei } Z_i \geq 6), \quad (19)$$

$$p_j^{mass} = (p_j^{Pauli} + p_j^{SE} + p_j^{Coul}) \quad (\text{light nuclei } Z_j \leq 5), \quad (20)$$

where $p_{p,n}^{RMF}$ is the contribution of the nucleons in the vapor; both $p_{i/j}^{th} = n_{i/j} k_B T (1 - n_B/n_s)$ and $p_{i/j}^{ex} = n_{i/j} k_B T (n_B/n_s) (\log(n_{i/j}/n_{Q_{i/j}}) - 1)$ come from the translational energy of nuclei in the free energy; p_i^{shell} , p_i^{Coul} and p_i^{Surf} originate from the shell, Coulomb and surface energies of heavy nuclei in the free energy, respectively; p_j^{Pauli} , p_j^{SE} (for d , t , h and α) and p_j^{Coul} are derived from the Pauli-, self- and Coulomb-energy shifts of the light nuclei.

The entropy per baryon is calculated from the following expression:

$$\begin{aligned} s &= - \frac{[\partial f / \partial T]_{\rho_B, Y_e}}{n_B}, \\ &= \eta_{p,n}^{RMF} + \sum_{i/j} \frac{n_{i/j} k_B}{n_B} \left[\left\{ \frac{5}{2} - \log \left(\frac{n_{i/j}}{g_{i/j} n_{Q_{i/j}}} \right) + \frac{\partial g_i(T)}{\partial T} / g_i(T) \right\} (1 - n_B/n_s) - \frac{\partial M_{i/j}}{\partial T} \right]. \end{aligned} \quad (21)$$

In the new model, the introduction of temperature-dependence of some in-medium effects yields the term of $\partial g_i(T) / \partial T / g_i(T)$ for heavy nuclei and contributes to the partial derivative of the masses, which are obtained as follows:

$$\frac{\partial M_i}{\partial T} = -A_i s_i^{RMF}(T, n_{si}, Z_i/A_i) + \frac{\partial E_i^{Su}}{\partial T} + \frac{\partial E_i^{Sh}}{\partial T} \quad (\text{heavy nuclei}) \quad (22)$$

$$\frac{\partial M_j}{\partial T} = \frac{\partial \Delta E_j^{SE}}{\partial T} + \frac{\partial \Delta E_j^{Pa}}{\partial T} \quad (\text{light nuclei } Z_j \leq 5), \quad (23)$$

where the entropy per baryon s_i^{RMF} is obtained by the RMF. The contribution of this term is normally negligible except near the nuclear saturation density.

3. Result

In this paper, we construct the EOS that improves the previous one (Furusawa et al., 2013). The changes are the additions of the temperature dependences in the surface and shell energies of heavy nuclei and the reformulation of the mass evaluation for the light nuclei other than d , t , h and α . We compare the results of the different models listed in Table 1, focusing on the impact of the improvements. Model 0f is the same EOS as the previous EOS (Furusawa et al., 2013), in which the binding energies of light nuclei $Z \leq 5$ other than d , t , h and α are calculated via the LDM. In other models, they are evaluated with the quasi-particle method as noted in Sec. 2.4. The temperature dependence in the surface energy given in Eq. (6) with the last factor $((T_c^2 - T^2)/(T_c^2 + T^2))^{5/4}$ is employed in Models 2f, 2w and 2n, whereas the factor is dropped in Models 0f and 1f. Models 0f, 1f and 2f ignore the washout of the shell effects, dropping the factor $\tau_i/\sinh\tau_i$ in Eq. (8). They may be regarded as a surrogate for HS EOS (Hempel and Schaffner-Bielich, 2010) and the ordinary NSE EOS (Timmes and Arnett, 1999), which also neglect the washout effect. Model 2w is the new EOS, in which we take this effect. We also prepare Model 2n for comparison, which do not consider the shell effects at all ($E_{i0}^{Sh} = 0$). This model is similar to the SMSM EOS, in which nuclei are described by the LDM description without shell effects. Note that the density dependence in the shell effects between $\rho_B = 10^{12} \text{g/cm}^3$ and ρ_0 in Eq. (8) is included in all the model although it is effective only near the saturation densities.

First, we will elucidate the difference between Models 0f and 1f, paying attention to the mass fraction of light nuclei. Then we discuss the impact of the temperature dependence of in-medium effects on the abundance of the heavy nuclei, based on the results of Models 1f, 2f, 2w and 2n. Finally, the thermodynamical quantities are compared for all models.

Figure 1 displays the mass fractions of proton, neutron, the light nuclei of d , t , h and α , the rest of light nuclei ($Z \leq 5$) as well as heavy nuclei ($Z \geq 6$) for Models 0f and 1f at $\rho_B = 10^{12} \text{g/cm}^3$ and $Y_p = 0.2$ and 0.4 as a function of temperature and those at $T = 3 \text{ MeV}$ and $Y_p = 0.2$ and 0.4 as a function of density. It is found that the mass fraction of the light nuclei other than d ,

t , h and α decreases in Model 1f compared with Model 0f due to the Pauli shifts. The reduction does not affect the mass fractions of free nucleons and the other nuclei take their place. The difference is apparently small, since these light nuclei are never dominant as already explained. The light nuclei in the pasta phase are also replaced by the heavy-nuclei pasta around $\rho \sim 10^{14}$ g/cm³ for $T = 3$ MeV and $Y_p = 0.2$. These changes have essentially no influence on thermodynamical quantities as shown later in Figs. 6 and 7.

Figures 2 and 3 show the mass fractions of elements as a function of the mass number for Models 1f, 2f, 2w and 2n at $\rho_B = 10^{12}$ g/cm³, $T = 0.5, 1.0, 2.0$ and 3.0 MeV and $Y_p = 0.2$ and 0.4 . We can see from the comparison of Models 1f and 2f that the temperature dependence in the surface energies has no influence on the nuclear abundance below $T = 1$ MeV. At $T = 2$ and 3 MeV, the population of small-mass number elements is larger in Model 2f than in Model 1f due to the reduction of surface tension. The temperature dependence in the shell effects affects more on the element distribution at low temperatures than that in the surface tension. It can be seen in Model 2w that the washout effect makes the element distributions smoother compared to the case with no washout (Model 2f). The differences are visible even at $T = 0.5$ MeV both for $Y_p = 0.2$ and 0.4 . We find that this effect reduces the mass fractions of nuclei in the vicinity of the neutron magic numbers $N = 28, 50, 82$ and 126 , which correspond to the peaks at $A \sim 50, 80, 120$ and 170 in the figures, respectively. It is evident that the peak at a larger mass number is more strongly suppressed since the energy spacing, ϵ_i^{sh} , is smaller for nuclei with larger mass numbers. For instance, the third peak disappears for $T = 1$ MeV and $Y_p = 0.4$. For $T = 2$ and 3 MeV, the shell effects are almost gone and there is no discernible feature remaining at the magic numbers in Model 2w as in Model 2n, in which no shell effect is taken into account.

The average mass number of heavy nuclei ($Z_i \geq 6$) is displayed in Fig. 4 at $\rho_B = 10^{12}$ g/cm³ and $Y_p = 0.2$ and 0.4 as a function of temperature and at $T = 3$ MeV, $Y_p = 0.2$ and $T = 1$ MeV, $Y_p = 0.4$ as a function of density. The difference between Models 1f and 2f indicates that the temperature dependence in the surface tension cuts down the mass number of nuclei above $T \sim 2$ MeV, which can be confirmed also in Figs. 2 and 3. The washout of shell effects tends to reduce the averaged mass number around $T \sim 1$ MeV for $\rho = 10^{12}$ g/cm³ and $Y_p = 0.2$ and 0.4 (top panels). This is due to the reduction of the third peak at $N = 82$ as explained in the previous paragraph. Models 2w and 2n become almost identical around $T \sim 3$ MeV, which means

the shell effects are completely extinct. At high densities for $T = 3$ MeV and $Y_p = 0.2$, we can see the average mass number in Model 2w is decreased by the temperature effects both in the surface and shell energies. Note that the decline of the average mass number around $\rho \sim 10^{14}$ g/cm³ for $T = 3$ MeV and $Y_p = 0.2$ is due to the formation of nuclear pastas as discussed in detail in the previous paper (Furusawa et al., 2011). It is interesting that for $T = 1$ MeV and $Y_p = 0.4$, Model 2w is essentially identical to Model 2f at low densities but gets closer to Model 2n at $\rho \gtrsim 10^{13.5}$ g/cm³. This is because the shell effects of nuclei with larger mass numbers are more likely to be washed out as already explained. It is also remarkable that the average mass number in Model 2w does not always settle down to a value between those in Models 2f and 2n, since the shell effects are sensitive to the nuclear species and the washout affects the average mass number nonlinearly.

The total mass fractions of the heavy nuclei are shown in Fig. 5 at $\rho_B = 10^{12}$ g/cm³ and $Y_p = 0.2$ and 0.4 as a function of temperature and at $T = 3$ MeV, $Y_p = 0.2$ and $T = 1$ MeV, $Y_p = 0.4$ as a function of density. The mass fraction in Model 2f is larger than that in Model 1f at high temperatures, since the reduction of surface tension increases the binding energies (or decreases the free energies) of heavy nuclei. On the other hand, the washout of shell effect in Model 2w cuts down their mass fraction for $\rho_B = 10^{12}$ g/cm³ and $Y_p = 0.2$ and 0.4 (upper panels). The densities, where heavy nuclei emerge, are also affected by the difference in the shell effects and are lower in the order of Models 2f, 2w, 2n as shown in the bottom panels.

Figure 6 shows the absolute values of baryonic pressure for all models at $\rho_B = 10^{12}$ g/cm³ and $Y_p = 0.2$ and 0.4 as a function of temperature and at $T = 3$ MeV, $Y_p = 0.2$ and $T = 1$ MeV, $Y_p = 0.4$ as a function of density. At low temperatures and high densities, the pressure is negative, since the Coulomb energies of heavy nuclei decreases by the compression (Furusawa et al., 2011, 2013). We can see that the pressure is hardly affected either by the modifications for the light nuclei other than d , t , h and α or by the introductions of the temperature dependences in the surface tension and shell effect. It is also the case for the entropy per baryon as shown in Fig. 7. It is slightly affected, however, by the difference in the mass fractions of nucleons and nuclei as displayed in Figs. 1 and 5.

4. Summary and Discussion

We have constructed the improved baryonic EOS with multi-nucleus for the use in the simulation of core-collapse supernovae. This EOS provides the abundance of various nuclei with various in-medium effects being taken into consideration at high densities and/or temperatures. The major improvement in the new EOS is the introduction of the washout of shell effects based on the single particle motion of nucleons outside the closed shell, which has been ignored in any EOS employed so far for supernova simulations. We have also added the temperature dependence in the surface tensions and replaced the mass formula by the liquid drop model for the light nuclei ($Z \leq 5$) other than d , t , h and α with the one based on the quasi-particle description.

The basic part of the the model is the same as that given in Furusawa et al. (2013). The model free energy density is constructed so that it should reproduce the ordinary NSE results at low densities and temperatures and make a continuous transition to the supra-nuclear density EOS obtained from the RMF with the TM1 parameter set. The free energy density of the nucleon vapor outside nuclei is also calculated by the same RMF. The contribution from heavy nuclei is evaluated with the original LDM, in which their bulk energies are obtained again via the same RMF and various in-medium effects are taken into account for the surface and Coulomb energies such as the existence of the pasta phase near the nuclear saturation density. The shell energies in the vacuum limit are obtained from either experimental or theoretical data. The light nuclei d , t , h and α are handled with the quantum approach, in which the self- and Pauli-energy shifts are taken into account.

We have compared the abundances of nuclei as well as the thermodynamical quantities obtained in different models for some combinations of density, temperature and proton fraction. In the new model, the mass fraction of the light nuclei other than d , t , h and α is reduced a little due to the Pauli energy shifts. The temperature dependence in the surface energies for heavy nuclei leads solely to smaller average mass numbers and larger fractions of them above $T \sim 2$ MeV than before. This is because the reduction of surface energies requires smaller Coulomb energies. We have found that the introduction of the washout of shell effects greatly changes the compositions. The shell effects are washed out slightly even at $T \sim 1$ MeV and almost disappear at $T \sim 2 - 3$ MeV. These results are consistent with the findings by Nishimura and Takano (2014). It has been also shown that the shell effects for nuclei with larger mass numbers are more strongly washed out because

of the smaller energy spacing among the shells. It has been found that the modifications to the model free energy in this paper have little influence on thermodynamical quantities such as pressure and entropy.

The model free energy in the new EOS still has room for further improvement, since there are many uncertainties in our phenomenological treatment of the in-medium effects. We may need to sophisticate the EOS for uniform nuclear matter, on which the evaluations of the free nucleons as well as bulk energies of heavy nuclei are based. In fact, the RMF with TM1 parameter set is known to have the symmetry energy of $J = 36.9$ MeV which is larger than the canonical value $29 \lesssim J \lesssim 35$ MeV (Tews et al., 2013). It is noted, however, that the TM1 set is known to reproduce excellent properties of the ground states of stable nuclei as well as unstable nuclei and to agree well with experimental data in studies of nuclei with deformed configuration and the giant resonances within the RPA formalism (Sugahara and Toki, 1994; Hirata et al., 1995; Ma et al., 1997, 2001). The employment of another EOS for uniform nuclear matter (Togashi and Takano, 2013) is indeed under progress. We would like to stress, however, that the new EOS constructed in this paper is more realistic than the previous one and that the changes in the element distribution made by the washout of shell effects may have a great impact on the weak interaction rate in the collapsing cores of massive stars. The systematical study of such effects is also underway.

Acknowledgments

S.F. gratefully acknowledges S. Nishimura, M. Takano, M. Hempel and I. Mishustin for their useful discussions. S.F. is supported by Japan Society for the Promotion of Science Postdoctoral Fellowships for Research Abroad. Some numerical calculations were carried out on PC cluster at Center for Computational Astrophysics, National Astronomical Observatory of Japan. This work is supported in part by the usage of supercomputer systems through the Large Scale Simulation Program (No. 15/16/-08) of High Energy Accelerator Research Organization (KEK) and Post-K Projects (hp160071, hp160211) at K-computer, RIKEN AICS as well as the computational resources provided by RCNP at Osaka University, YITP at Kyoto University, University of Tokyo and JLDG. This work was supported by Grant-in-Aid for the Scientific Research from the Ministry of Education, Culture, Sports, Science and Technology (MEXT), Japan (24103006, 24244036, 16H03986, 15K05093, 24105008, 26104006).

Appendix: Table data

Our EOS tables are available on the Web at <http://user.numazu-ct.ac.jp/~sumi/eos/>. Below we explain the detailed information. The grid points and spacing for T , Y_p and ρ_B are just the same as those of Shen et al. (2011), which is summarized in Table 2. The results in the order of increasing Y_p and ρ_B are listed for each T . The temperature and its logarithm, $\log_{10}(T)$, in units of MeV are written at the beginning of the each block. The quantities in one line defined as follows:

1. Logarithm of baryon mass density: $\log_{10}(\rho_B)$ [g/cm³] ($\rho_B = n_B m_u$)
2. Baryon number density: n_B [fm⁻³]
3. Proton Fraction: Y_p
4. Free energy: $F = f/n_B - M_B$ [MeV]
5. Internal energy per baryon: $E_{int} = f/n_B - sT - m_u$ [MeV]
6. Entropy per baryon: s [k_B]
7. Average mass number of the heavy nuclei ($Z \geq 6$): $\langle A_i \rangle$
8. Average proton number of the heavy nuclei ($Z \geq 6$): $\langle Z_i \rangle$
9. Effective mass: m^* [MeV]
10. Free neutron fraction: X_n
11. Free proton fraction: X_p
12. Fraction of the light nuclei ($Z \leq 5$): X_a
13. Fraction of the heavy nuclei ($Z \geq 6$): X_A
14. Baryon Pressure: p_B [MeV/fm⁻³]
15. Chemical potential of the neutron: $\mu_n = (\partial f / \partial \tilde{n}_n)_{\tilde{n}_p} - m_B$ [MeV]
($\tilde{n}_n = (1 - Y_p)n_B$ and $\tilde{n}_p = Y_p n_B$)
16. Chemical potential of the proton: $\mu_p = (\partial f / \partial \tilde{n}_p)_{\tilde{n}_n} - m_B$ [MeV]
17. Average mass number of the light nuclei ($Z \leq 5$): $\langle A_j \rangle$
18. Average proton number of the light nuclei ($Z \leq 5$): $\langle Z_j \rangle$
19. Deuteron fraction: X_d
20. Triton fraction: X_t
21. Helion fraction: X_h
22. Alpha-particle fraction: X_α
23. Fraction of the light nuclei other than d , t , h and α ($Z \leq 5$): $X_{a'}$
($X_a = X_{a'} + X_d + X_t + X_h + X_\alpha$)
24. Average mass number of the light nuclei other than d , t , h and α ($Z \leq 5$): $\langle A_{j'} \rangle$
25. Average proton number of the light nuclei other than d , t , h and α ($Z \leq 5$): $\langle Z_{j'} \rangle$

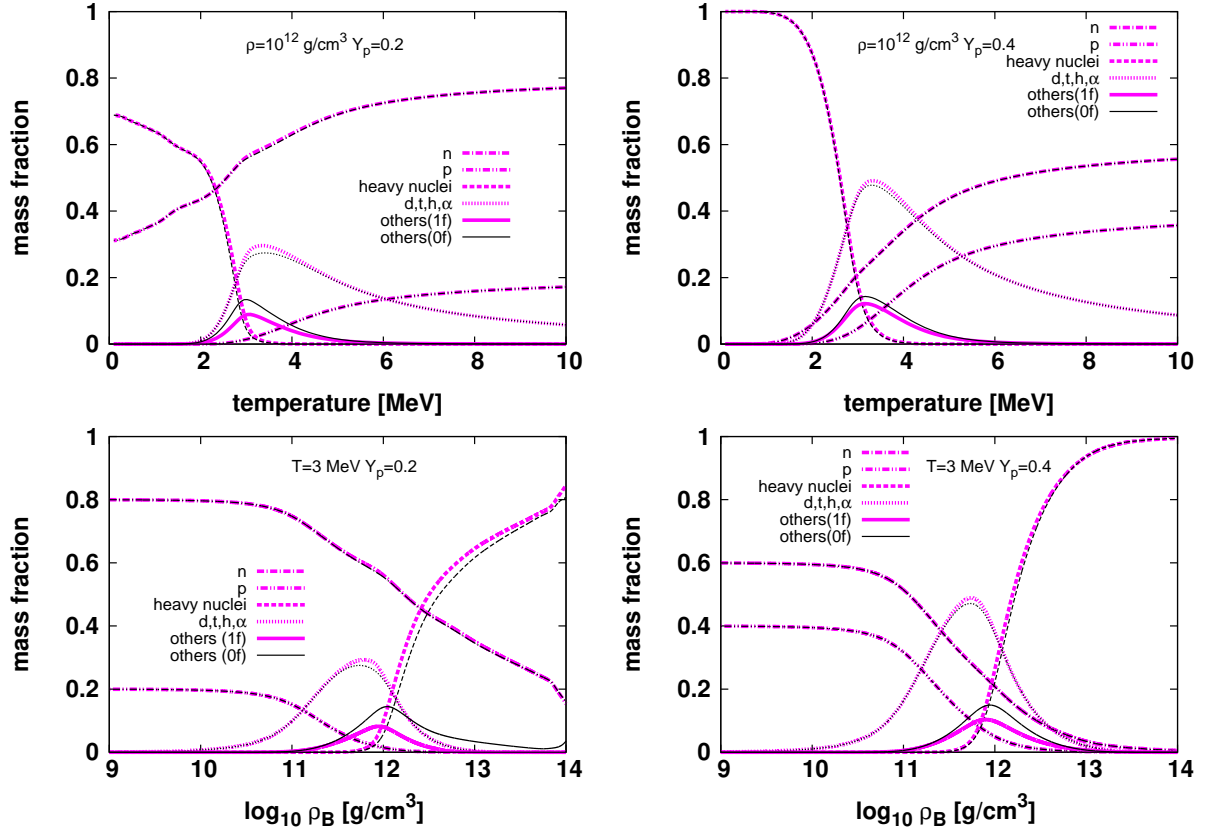


Figure 1: Mass fractions of neutrons (dash dotted lines), protons (dashed double-dotted lines), heavy nuclei with $Z \geq 6$ (dashed lines), d, t, h, α (dotted lines), the rest of light nuclei with $Z \leq 6$ (solid lines) for Models 1f (magenta lines) and 0f (black lines), respectively, at $Y_p = 0.2$ (left top panel) and 0.4 (right top panel) and $\rho_B = 10^{12} \text{ g/cm}^3$ as a function of temperature as well as at $T = 3 \text{ MeV}$ and $Y_p = 0.2$ (left bottom panel) and 0.4 (right bottom panel) as a function of density.

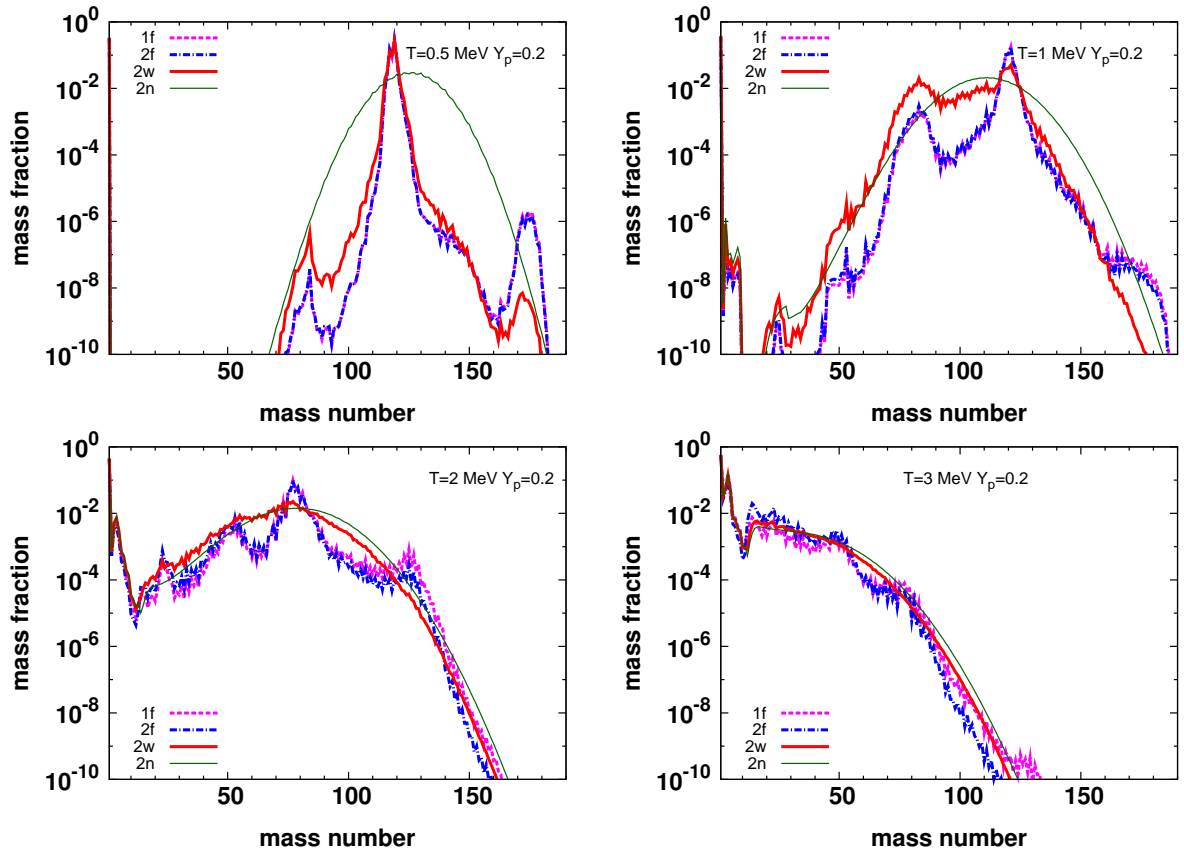


Figure 2: The mass fractions of elements as a function of the mass number for Models 1f (magenta dashed lines), 2f (blue dash dotted lines), 2w (red solid thick lines), 2n (green solid thin lines) at $T = 0.5$ (left top panel), 1.0 (right top panel), 2.0 (left bottom panel) and 3.0 (right bottom panel) MeV, $\rho_B = 10^{12}$ g/cm³ and $Y_p = 0.2$.

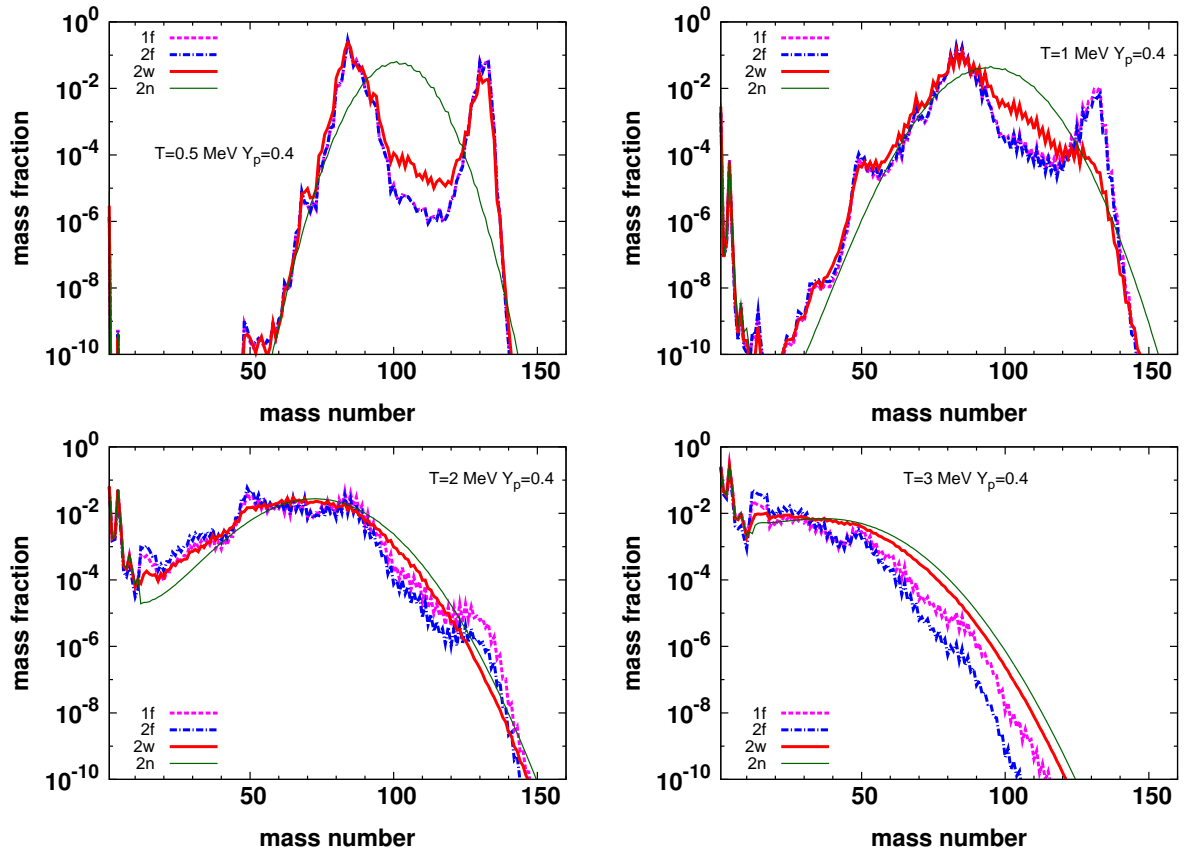


Figure 3: The mass fractions of elements as a function of the mass number for Models 1f (magenta dashed lines), 2f (blue dash dotted lines), 2w (red solid thick lines), 2n (green solid thin lines) at $T = 0.5$ (left top panel), 1.0 (right top panel), 2.0 (left bottom panel) and 3.0 (right bottom panel) MeV, $\rho_B = 10^{12}$ g/cm³ and $Y_p = 0.4$.

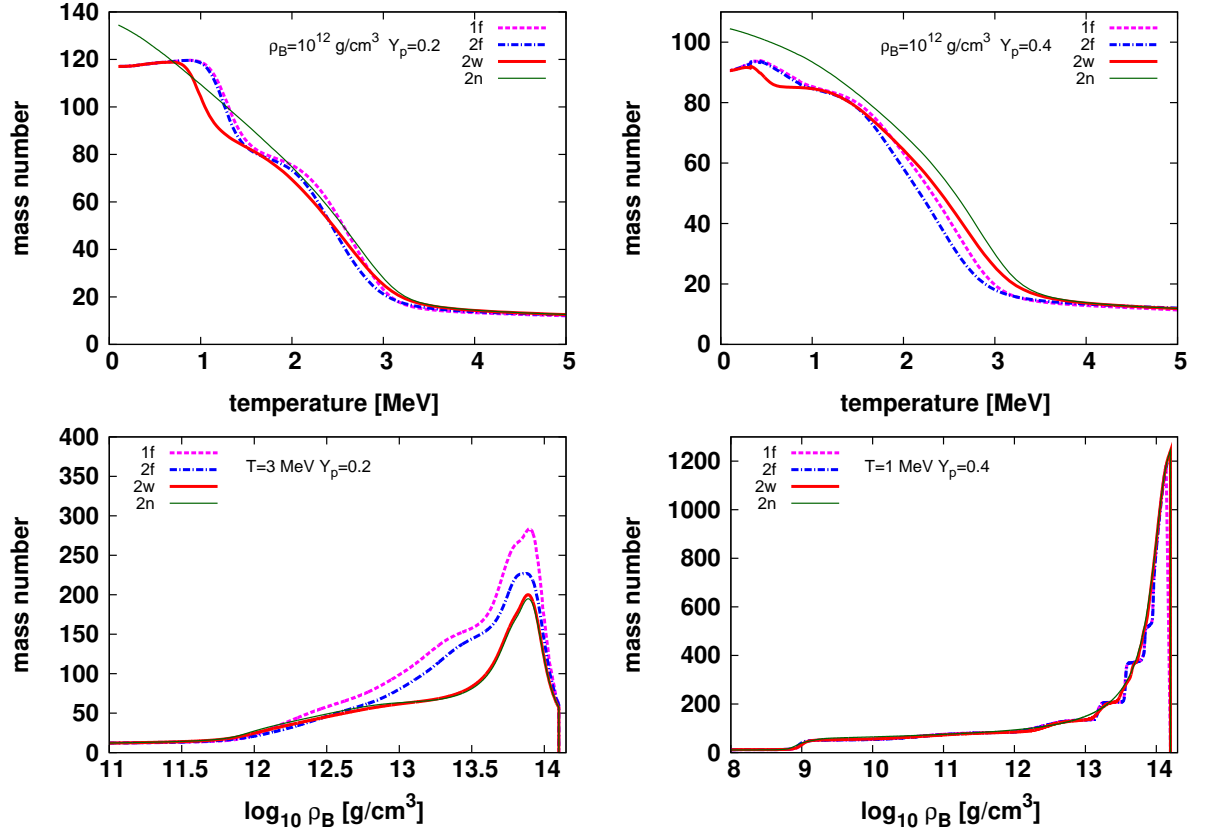


Figure 4: Average mass number of heavy nuclei with $Z \geq 6$ for for Models 1f (magenta dashed lines), 2f (blue dash dotted lines), 2w (red solid thick lines), 2n (green solid thin lines) at $Y_p = 0.2$ (left top panel) and 0.4 (right top panel) and $\rho_B = 10^{12} \text{ g/cm}^3$ as a function of temperature as well as at $T = 3 \text{ MeV}$ and $Y_p = 0.2$ (left bottom panel) and $T = 1 \text{ MeV}$ and $Y_p = 0.4$ (right bottom panel) as a function of density.

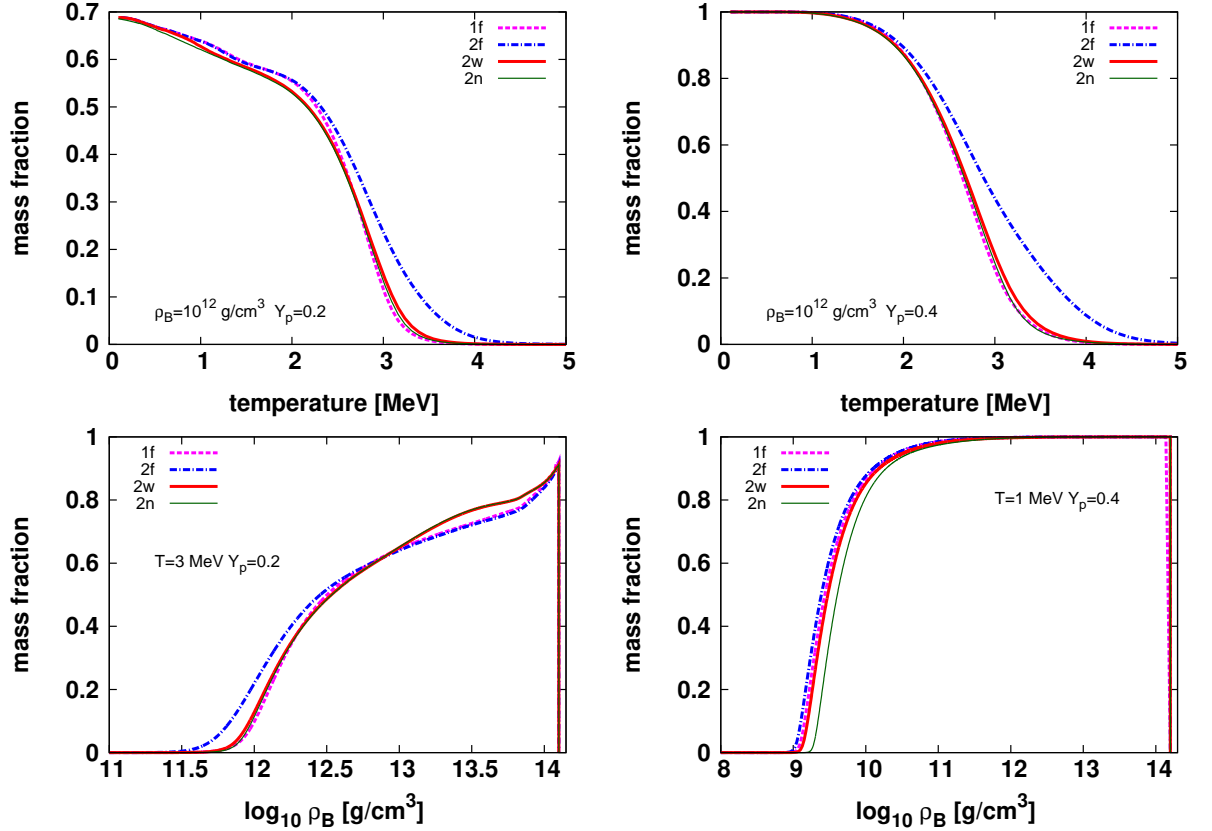


Figure 5: Mass fractions of heavy nuclei with $Z \geq 6$ for for Models 1f (magenta dashed lines), 2f (blue dash dotted lines), 2w (red solid thick lines), 2n (green solid thin lines) at $Y_p = 0.2$ (left top panel) and 0.4 (right top panel) and $\rho_B = 10^{12} \text{ g/cm}^3$ as a function of temperature as well as at $T = 3 \text{ MeV}$ and $Y_p = 0.2$ (left bottom panel) and $T = 1 \text{ MeV}$ and $Y_p = 0.4$ (right bottom panel) as a function of density.

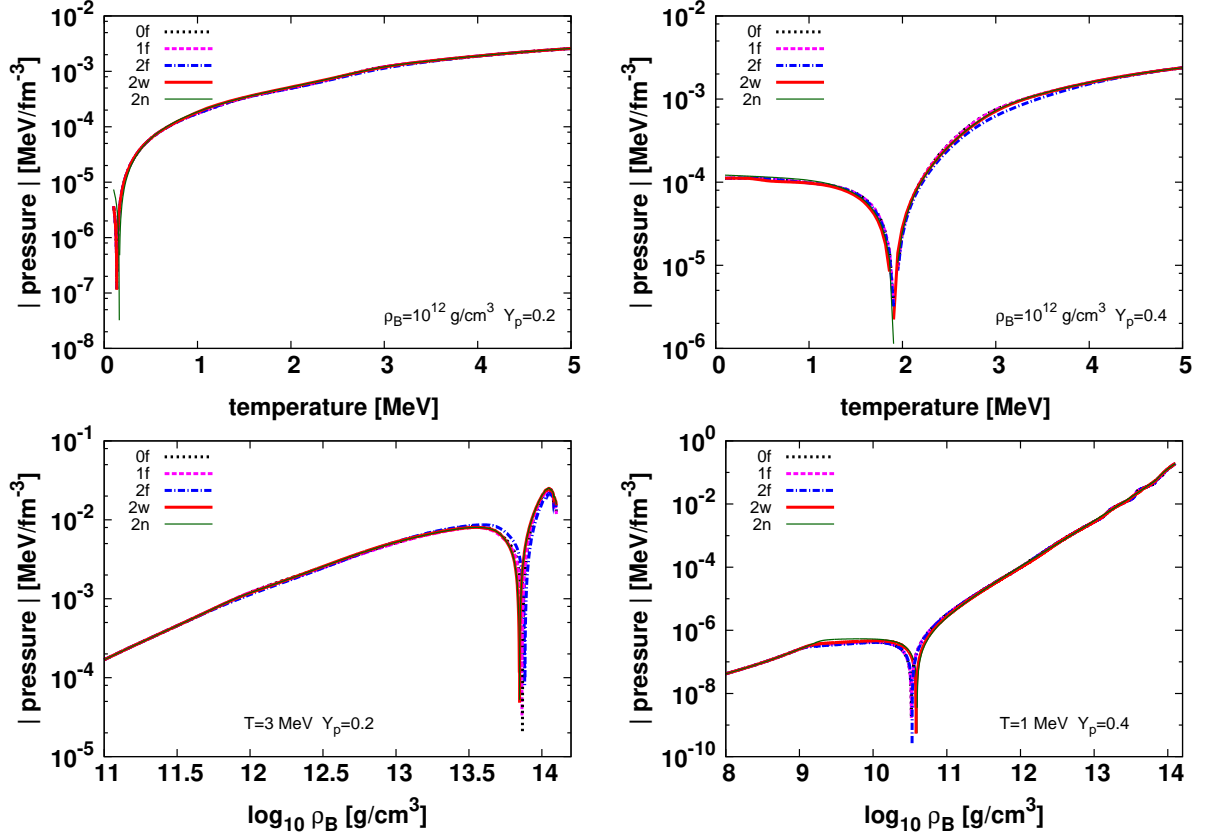


Figure 6: Absolute value of baryonic pressure for Models 0f (black dotted lines), 1f (magenta dashed lines), 2f (blue dash dotted lines), 2w (red solid thick lines), 2n (green solid thin lines) at $Y_p = 0.2$ (left top panel) and 0.4 (right top panel) and $\rho_B = 10^{12} \text{ g/cm}^3$ as a function of temperature as well as at $T = 3 \text{ MeV}$ and $Y_p = 0.2$ (left bottom panel) and $T = 1 \text{ MeV}$ and $Y_p = 0.4$ (right bottom panel) as a function of density.

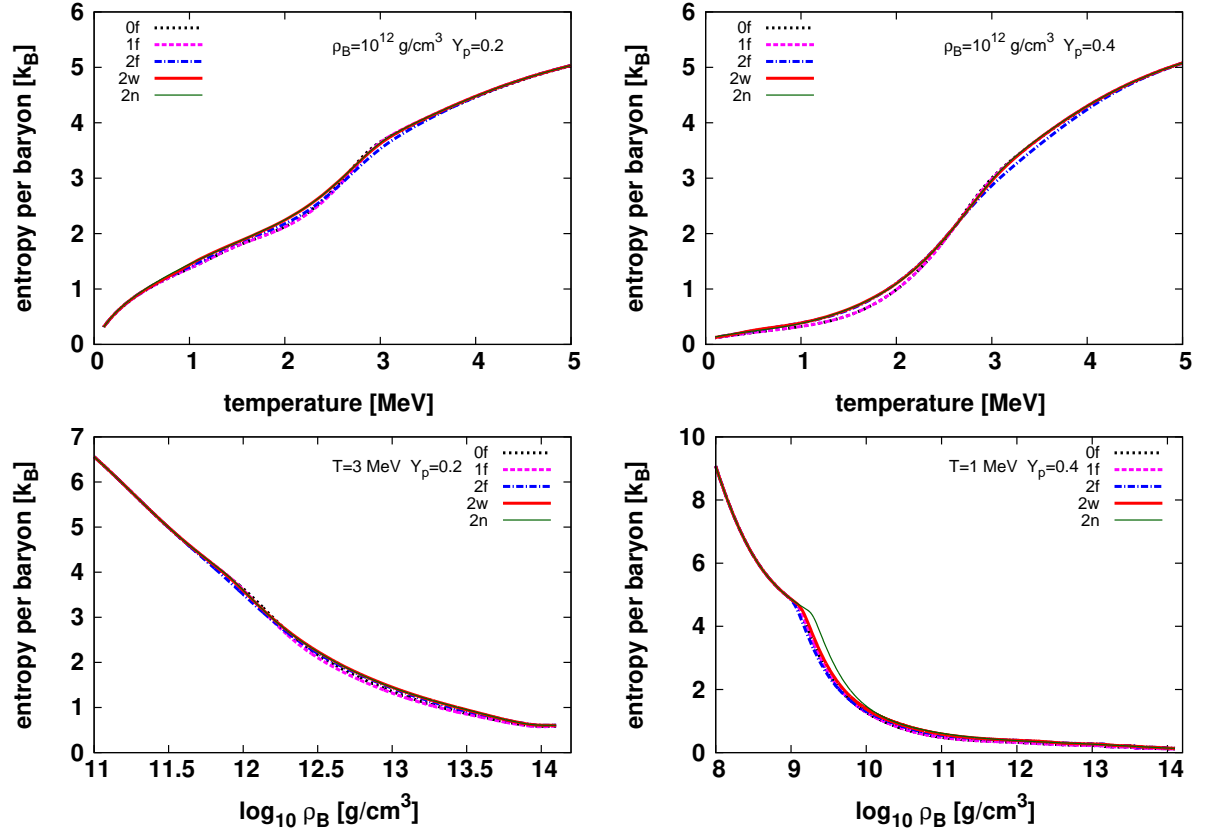


Figure 7: Entropy per baryon for Models 0f (black dotted lines), 1f (magenta dashed lines), 2f (blue dash dotted lines), 2w (red solid thick lines), 2n (green solid thin lines) at $Y_p = 0.2$ (left top panel) and 0.4 (right top panel) and $\rho_B = 10^{12} \text{ g/cm}^3$ as a function of temperature as well as at $T = 3 \text{ MeV}$ and $Y_p = 0.2$ (left bottom panel) and $T = 1 \text{ MeV}$ and $Y_p = 0.4$ (right bottom panel) as a function of density.

model	light nuclei other than d, t, h, α	T dependence in surface energies	shell energies	version
0f	LDM	no	full	FYSS13
1f	quasi-particle	no	full	
2f	quasi-particle	yes	full	
2w	quasi-particle	yes	washout	FYSS16
2n	quasi-particle	yes	no	

Table 1: Different models for comparisons. See the beginning of Sec. 3.

	Range	Grid spacing	Points
T	$-1.0 \leq \log_{10}(T) \leq 2.6$	$\Delta \log_{10}(T) = 0.04$	91
Y_p	$0.01 \leq Y_p \leq 0.65$	0.01	65
ρ_B	$5.1 \leq \log_{10} \rho_B \leq 16.0$	$\Delta \log_{10} \rho_B = 0.1$	110

Table 2: The EOS table of Model 2w (the same format as that of Shen et al. (2011)).

References

- Agrawal, B. K., De, J. N., Samaddar, S. K., Centelles, M., Viñas, X., Feb. 2014. Symmetry energy of warm nuclear systems. *European Physical Journal A* 50, 19.
- Audi, G., M., W., A. H., W., F. G., K., MacCormick, M., Xu, X., Pfeiffer, B., Dec. 2012. The Ame2012 atomic mass evaluation. *Chinese Physics C* 36, 002.
- Aymard, F., Gulminelli, F., Margueron, J., Jun. 2014. In-medium nuclear cluster energies within the extended Thomas-Fermi approach. *Phys. Rev. C* 89 (6), 065807.
- Blinnikov, S. I., Panov, I. V., Rudzsky, M. A., Sumiyoshi, K., Nov. 2011. The equation of state and composition of hot, dense matter in core-collapse supernovae. *Astronomy & Astrophysics* 535, A37.
- Bohr, A., Mottelson, B., 1998. *Nuclear Structure*. No. v. 2 in *Nuclear Structure*. World Scientific.
URL <https://books.google.com.au/books?id=11pshSMQwcYC>

- Bondorf, J. P., Botvina, A. S., Iljinov, A. S., Mishustin, I. N., Sneppen, K., Jun. 1995. Statistical multifragmentation of nuclei. *Physics Reports* 257, 133–221.
- Botvina, A. S., Mishustin, I. N., Apr. 2004. Formation of hot heavy nuclei in supernova explosions. *Physics Letters B* 584, 233–240.
- Botvina, A. S., Mishustin, I. N., Oct. 2010. Statistical approach for supernova matter. *Nuclear Physics A* 843, 98–132.
- Brack, M., Quentin, P., Sep. 1974. Selfconsistent calculations of highly excited nuclei. *Physics Letters B* 52, 159–162.
- Burrows, A., Jan. 2013. Colloquium: Perspectives on core-collapse supernova theory. *Reviews of Modern Physics* 85, 245–261.
- Burrows, A., Lattimer, J. M., Oct. 1984. On the accuracy of the single-nucleus approximation in the equation of state of hot, dense matter. *Astrophys. J.* 285, 294–303.
- Buyukcizmeci, N., Botvina, A. S., Mishustin, I. N., Jul. 2014. Tabulated Equation of State for Supernova Matter Including Full Nuclear Ensemble. *Astrophys. J.* 789, 33.
- Buyukcizmeci, N., Botvina, A. S., Mishustin, I. N., Ogul, R., Hempel, M., Schaffner-Bielich, J., Thielemann, F.-K., Furusawa, S., Sumiyoshi, K., Yamada, S., Suzuki, H., Jun. 2013. A comparative study of statistical models for nuclear equation of state of stellar matter. *Nuclear Physics A* 907, 13–54.
- Furusawa, S., Sumiyoshi, K., Yamada, S., Suzuki, H., Aug. 2013. New Equations of State Based on the Liquid Drop Model of Heavy Nuclei and Quantum Approach to Light Nuclei for Core-collapse Supernova Simulations. *Astrophys. J.* 772, 95.
- Furusawa, S., Yamada, S., Sumiyoshi, K., Suzuki, H., Sep. 2011. A New Baryonic Equation of State at Sub-nuclear Densities for Core-collapse Simulations. *Astrophys. J.* 738, 178.
- Hempel, M., Schaffner-Bielich, J., Jun. 2010. A statistical model for a complete supernova equation of state. *Nuclear Physics A* 837, 210–254.

- Hirata, D., Toki, H., Tanihata, I., Feb. 1995. Relativistic mean-field theory on the xenon, cesium and barium isotopes. *Nuclear Physics A* 589, 239–248.
- Hix, W. R., Messer, O. E., Mezzacappa, A., Liebendörfer, M., Sampaio, J., Langanke, K., Dean, D. J., Martínez-Pinedo, G., Nov. 2003. Consequences of Nuclear Electron Capture in Core Collapse Supernovae. *Physical Review Letters* 91 (20), 201102.
- Janka, H.-T., Nov. 2012. Explosion Mechanisms of Core-Collapse Supernovae. *Annual Review of Nuclear and Particle Science* 62, 407–451.
- Kotake, K., Takiwaki, T., Suwa, Y., Iwakami Nakano, W., Kawagoe, S., Masada, Y., Fujimoto, S.-i., 2012. Multimessengers from Core-Collapse Supernovae: Multidimensionality as a Key to Bridge Theory and Observation. *Advances in Astronomy* 2012, 428757.
- Koura, H., Tachibana, T., Uno, M., Yamada, M., Feb. 2005. Nuclidic Mass Formula on a Spherical Basis with an Improved Even-Odd Term. *Progress of Theoretical Physics* 113, 305–325.
- Lattimer, J. M., Swesty, F. D., Dec. 1991. A generalized equation of state for hot, dense matter. *Nuclear Physics A* 535, 331–376.
- Lentz, E. J., Mezzacappa, A., Messer, O. E. B., Hix, W. R., Bruenn, S. W., Nov. 2012. Interplay of Neutrino Opacities in Core-collapse Supernova Simulations. *Astrophys. J.* 760, 94.
- Ma, Z., Toki, H., Chen, B., Giai, N. V., Oct. 1997. The Giant Dipole Resonance in Ar-Isotopes in the Relativistic RPA. *Progress of Theoretical Physics* 98, 917–926.
- Ma, Z.-y., Van Giai, N., Wandelt, A., Vretenar, D., Ring, P., Apr. 2001. Isoscalar compression modes in relativistic random phase approximation. *Nuclear Physics A* 686, 173–186.
- Newton, W. G., Stone, J. R., May 2009. Modeling nuclear “pasta” and the transition to uniform nuclear matter with the 3D Skyrme-Hartree-Fock method at finite temperature: Core-collapse supernovae. *Phys. Rev. C* 79 (5), 055801.

- Nishimura, S., Takano, M., May 2014. Shell effects in hot nuclei and their influence on nuclear composition in supernova matter. In: Jeong, S., Imai, N., Miyatake, H., Kajino, T. (Eds.), American Institute of Physics Conference Series. Vol. 1594 of American Institute of Physics Conference Series. pp. 239–244.
- Okamoto, M., Maruyama, T., Yabana, K., Tatsumi, T., Jul. 2012. Three-dimensional structure of low-density nuclear matter. *Physics Letters B* 713, 284–288.
- Raduta, A. R., Gulminelli, F., Oertel, M., Feb. 2016. Modification of magicity toward the dripline and its impact on electron-capture rates for stellar core collapse. *Phys. Rev. C* 93 (2), 025803.
- Ravenhall, D. G., Pethick, C. J., Wilson, J. R., Jun. 1983. Structure of Matter below Nuclear Saturation Density. *Physical Review Letters* 50, 2066–2069.
- Röpke, G., Jan. 2009. Light nuclei quasiparticle energy shifts in hot and dense nuclear matter. *Phys. Rev. C* 79 (1), 014002.
- Sandulescu, N., Civitarese, O., Liotta, R. J., Vertse, T., Mar. 1997. Effects due to the continuum on shell corrections at finite temperatures. *Phys. Rev. C* 55, 1250–1254.
- Shen, G., Horowitz, C. J., Teige, S., Mar. 2011. New equation of state for astrophysical simulations. *Phys. Rev. C* 83 (3), 035802.
- Shen, H., Toki, H., Oyamatsu, K., Sumiyoshi, K., Jul. 1998a. Relativistic equation of state of nuclear matter for supernova and neutron star. *Nuclear Physics A* 637, 435–450.
- Shen, H., Toki, H., Oyamatsu, K., Sumiyoshi, K., Nov. 1998b. Relativistic Equation of State of Nuclear Matter for Supernova Explosion. *Progress of Theoretical Physics* 100, 1013–1031.
- Shen, H., Toki, H., Oyamatsu, K., Sumiyoshi, K., 2011. Relativistic Equation of State for Core-Collapse Supernova Simulations. *Astrophys.J.Suppl.* 197, 20.
- Steiner, A. W., Hempel, M., Fischer, T., Sep. 2013. Core-collapse Supernova Equations of State Based on Neutron Star Observations. *Astrophys. J.* 774, 17.

- Sugahara, Y., Toki, H., 1994. Relativistic mean field theory for unstable nuclei with nonlinear sigma and omega terms. Nucl.Phys. A579, 557–572.
- Tews, I., Krüger, T., Hebeler, K., Schwenk, A., Jan 2013. Neutron matter at next-to-next-to-next-to-leading order in chiral effective field theory. Phys. Rev. Lett. 110, 032504.
URL <http://link.aps.org/doi/10.1103/PhysRevLett.110.032504>
- Timmes, F. X., Arnett, D., Nov. 1999. The Accuracy, Consistency, and Speed of Five Equations of State for Stellar Hydrodynamics. Astrophys.J.Suppl125, 277–294.
- Togashi, H., Takano, M., Mar. 2013. Variational study for the equation of state of asymmetric nuclear matter at finite temperatures. Nuclear Physics A 902, 53–73.
- Typel, S., Röpke, G., Klähn, T., Blaschke, D., Wolter, H. H., Jan. 2010. Composition and thermodynamics of nuclear matter with light clusters. Phys. Rev. C81 (1), 015803.
- Watanabe, G., Maruyama, T., Sato, K., Yasuoka, K., Ebisuzaki, T., Jan. 2005. Simulation of Transitions between “Pasta” Phases in Dense Matter. Physical Review Letters 94 (3), 031101.